Available online at www.sciencedirect.com

International Journal of Solids and Structures 43 (2006) 3381–3400

www.elsevier.com/locate/ijsolstr

A Galerkin method for distributed systems with non-local damping

Y. Lei [a], M.I. Friswell [b,*], S. Adhikari [b]

[a] College of Aerospace and Material Engineering, National University of Defense Technology, Changsha, Hunan 410073, PR China
[b] Department of Aerospace Engineering, University of Bristol, Queen's Building, University Walk, Bristol BS8 1TR, UK

Received 20 February 2005; received in revised form 19 June 2005
Available online 18 August 2005

Abstract

In this paper, a non-local damping model including time and spatial hysteresis effects is used for the dynamic analysis of structures consisting of Euler–Bernoulli beams and Kirchoff plates. Unlike ordinary local damping models, the damping force in a non-local model is obtained as a weighted average of the velocity field over the spatial domain, determined by a kernel function based on distance measures. The resulting equation of motion for the beam or plate structures is an integro-partial-differential equation, rather than the partial-differential equation obtained for a local damping model. Approximate solutions for the complex eigenvalues and modes with non-local damping are obtained using the Galerkin method. Numerical examples demonstrate the efficiency of the proposed method for beam and plate structures with simple boundary conditions, for non-local and non-viscous damping models, and different kernel functions.

Keywords: Non-local damping; Galerkin; Beam; Plate

1. Introduction

The dynamic response analysis of damped structures is important in many areas of mechanical, civil and aerospace engineering, such as the vibration isolation of precise equipment, aircraft noise, or the vibration of cable stayed bridges. Although the damping model plays a key role in the dynamic analysis, particularly for complex structures, this model is often approximated by classical or proportional damping distributions

* Corresponding author. Tel.: +44 (0) 117 928 8695; fax: +44 (0) 117 927 2771.
E-mail address: m.i.friswell@bristol.ac.uk (M.I. Friswell).

0020-7683/$ - see front matter
doi:10.1016/j.ijsolstr.2005.06.058

for convenience. In many practical situations this simplified approach does not describe the dynamics of the structure with sufficient accuracy because of the complicated damping mechanisms that occur in practice. Theoretically speaking, any model that makes the energy dissipation function non-negative is a possible candidate for a valid damping model. There are many damping models, and determining a unified damping model for real engineering systems is difficult, and approximations are generally used. For single degree-of-freedom (SDOF) dynamic systems three common damping models are viscous, structural and Coulomb friction damping. However, for the analysis of multi degree-of-freedom (MDOF) damped systems or a distributed system the most popular model is viscous damping, first introduced by Rayleigh in 1877. Often proportional damping is assumed.

Recently, non-proportional damping models have been proposed and studied. Yang and Wu (1997) studied the transient response of general one-dimensional distributed systems with viscous damping by the transfer function method, and computed complex eigenvalues and modes. To control structural vibration, the application of discrete dampers is popular in engineering practice. Krenk (2004) investigated the complex eigenproblem of cables or beams with a viscous damper at the boundary or at an intermediate position. Krenk and Hogsberg (2005) further investigated the modal response of a cable with transverse dampers modelled with viscous, viscoelastic, fractionally viscous or nonlinearly viscous properties. The damping models in the work of Krenk and his co-workers were non-proportional, and they demonstrated that the eigenvalues corresponding to vibration modes were located on a circular arc in the complex plane. Sorrentino et al. (2003) proposed a state-space solution for one-dimensional distributed systems by the transfer matrix method, where the damping arose from external viscosity or internal structural dissipation.

Other authors have generalised the damping model from viscous to non-viscous. Adhikari (2000, 2001) and Adhikari and Woodhouse (2001) presented a systematic study on the analysis and identification of damped mechanical systems, focused on non-viscously damped MDOF linear vibrating systems. Woodhouse (1998) obtained approximate expressions for damped natural frequencies, complex modes and transfer functions for linear systems with light viscous and non-viscous damping. Podlubny (1999) and Mainardi (1997) used fractional derivative constitutive models, based on fractional differential theory, to describe the damping behaviour of viscoelastic materials. Bagley and Torvik (1983, 1985) presented a finite element formulation and closed form solutions in the Laplace domain for the dynamics of damped bar and beam structures. They showed that the fractional derivative model has some attractive features, and that very few empirical parameters are required to model the viscoelastic material over a wide range frequency. Enelund and Josefson (1997) developed a time domain finite element approach for the dynamic analysis of structures with viscoelastic material modelled using the fractional derivative approach. Maia et al. (1998) used a fractional derivative damping model to analyse the dynamic characteristics of SDOF and MDOF vibration systems. Agrawal (2004) used a normal mode approach to obtain the analytical solution for the stochastic response of a simply supported beam with external damping modelled using fractional derivatives. Atanackovic and Stankovic (2004) analysed the dynamic stability of a rod resting on a viscoelastic soil foundation. Fenander (1998) investigated the dynamic behaviour of a railway track with a fractional derivative railpad model, although the foundation model was local in the sense that the force at a point only depended on the deformations at that same point.

Flugge (1975) argued in his text book of *Viscoelasticity*, that:

"The reaction $q(x_1)$ at any point x_1, of course, not only depends upon the local value $w(x_1)$ of the deflection, but also upon that of neighbour points x_2, their influence decreasing as the distance $|x_1 - x_2|$ increases".

Thus the practical needs of engineering problems motivate the study of non-local models. In physical terms the non-local damping or elasticity property often arises when two-dimensional structures are modelled as one-dimensional. For example, classical beam theory assumes that plane sections remain plane, however complex deformations of the beam section will mean that deformations at one position along a beam will produce forces and moments at other points in the beam.

In this paper we consider a new non-local damping model to analyse the dynamic characteristics of an Euler–Bernoulli beam with different boundary conditions. The model is also applied to the dynamic analysis of simply supported Kirchoff (i.e. thin) plates. The non-local damping model is a generalisation of viscous damping and it has many potential applications in engineering structures with non-local energy dissipation mechanisms. Examples include structures with viscoelastic damping layer treatments, structures supported on viscoelastic foundations, long adhesive joints in composites and surface damping treatments for vibration suppression using fluids (Ghoneim, 1997). Russell (1992) first proposed a non-local damping model for the vibration analysis of a composite beam with an internal damping torque. Eringen and Edelen (1972) introduced a non-local elasticity model and this was further analysed by Polizzotto (2001) and Pisno and Fuschi (2003). Silling et al. (2003) and Weckner and Abeyaratne (2005) recently used a displacement-difference-based non-local model to analyse the peridynamic problem involving long-range force effects in an elastic medium. Based on the non-local elasticity theory, Ahmadi (1975) was the first to suggest a model of non-local viscoelasticity. Nowinski (1986) established the fundamental equations for the propagation of plane longitudinal harmonic waves in Voigt–Kevin and Maxwell media.

Banks and Inman (1991) considered four different damping models for composite beams, namely viscous air damping, Kelvin–Voigt damping, time hysteresis damping and spatial hysteresis damping. The spatial hysteresis damping model may be treated as a non-local damping model and its non-local parameters estimated. The spatial hysteresis model, combined with viscous air damping, gave the best quantitative agreement with experimental time histories. Lin and Russell (2001) investigated the convergence of the bending moment for an elastic beam with spatial hysteresis damping.

The non-local models mentioned above are mainly devoted to theoretical aspects of the non-locally damped system. The complex eigenvalues and modes were generally not computed, and the influence of the non-local damping models on the modal characteristics has not been investigated. Recently, Adhikari et al. (submitted for publication) presented a closed form solution for a beam with non-local damping using a transfer function method for the distributed parameter system (Yang and Tan, 1992). However, solutions were only possible for special cases of the spatial kernel function, and the influence of different kernel functions on the dynamic characteristics were not investigated. In this paper, several kernel functions are considered that describe possible models of the non-local effect of material damping. These models are analysed to demonstrate the influence of the kernel functions on the complex eigenvalues and modes.

2. The non-local damping model

In this section, a general non-local damping model for distributed parameter dynamic systems is proposed. This damping model assumes that the damping force at a given point depends on the past history of a velocity field over a certain domain, through a kernel function. The governing equation of motion for a linear damped continuous dynamic system may be expressed in operator form as

$$\rho(\mathbf{r})\ddot{\mathbf{u}}(\mathbf{r},t) + (L_{\mathrm{e}} + L_{\mathrm{i}})\dot{\mathbf{u}}(\mathbf{r},t) + L_{\mathrm{k}}\mathbf{u}(\mathbf{r},t) = \mathbf{f}(\mathbf{r},t) \quad \text{for } \mathbf{r} \in \Omega, \quad t \in [0,T], \tag{1}$$

where $\mathbf{u}(\mathbf{r},t)$ is the displacement vector, $\mathbf{r}$ is the spatial position vector, t is time, $\rho(\mathbf{r})$ is the distributed mass density, and $\mathbf{f}(\mathbf{r},t)$ is the distributed external load. L_{e} and L_{i} are the external and internal damping operators, respectively. L_{k} is the spatial self-adjoint stiffness operator.

In this paper, the following special forms are used for the damping operators L_{e} and L_{i},

$$L_{\mathrm{e}}\dot{\mathbf{u}}(\mathbf{r},t) = \int_{\Omega}\int_0^t C_{\mathrm{e}}(\mathbf{r},\xi,t-\tau)\dot{\mathbf{u}}(\xi,\tau)\,\mathrm{d}\tau\,\mathrm{d}\xi, \tag{2a}$$

$$L_{\mathrm{i}}\dot{\mathbf{u}}(\mathbf{r},t) = \int_{\Omega}\int_0^t C_i(\mathbf{r},\xi,t-\tau)L_{\mathrm{s}}\dot{\mathbf{u}}(\xi,\tau)\,\mathrm{d}\tau\,\mathrm{d}\xi, \tag{2b}$$

where $C_e(\mathbf{r}, \xi, t-\tau)$ and $C_i(\mathbf{r}, \xi, t-\tau)$ are the kernel functions for the external and internal damping respectively. The internal and external damping are treated differently because the external damping is only dependent on the displacement, whereas the internal damping is dependent on the internal strains, which are given by spatial derivatives of the displacement through the operator L_s. The stiffness operator in Eq. (1), L_k, may be treated in a similar way when the distributed parameter dynamic system has non-local elastic or viscoelastic material. In this paper we only consider the non-local influence of the damping operators, L_e and L_i, although the extension to stiffness is straight-forward.

Eq. (1) is subject to the following initial and boundary conditions:

$$\mathbf{u}(\mathbf{r}, 0) = \bar{\mathbf{u}}(\mathbf{r}), \qquad \left.\frac{\partial \mathbf{u}(\mathbf{r}, t)}{\partial t}\right|_{t=0} = \bar{\mathbf{v}}(\mathbf{r}), \tag{3}$$

$$M_1\mathbf{u}(\mathbf{r}, t) = \bar{\mathbf{g}}_1(\mathbf{r}, t) \text{ for } \mathbf{r} \in \Gamma_1 \quad \text{and} \quad M_2\mathbf{u}(\mathbf{r}, t) = \bar{\mathbf{g}}_2(\mathbf{r}, t) \text{ for } \mathbf{r} \in \Gamma_2, \tag{4}$$

where $\bar{\mathbf{u}}(\mathbf{r})$ and $\bar{\mathbf{v}}(\mathbf{r})$ are the initial displacement and velocity, M_1 and M_2 are spatial operators, Γ_1 and Γ_2 are the boundary domains, and $\bar{\mathbf{g}}_1(\mathbf{r}, t)$ and $\bar{\mathbf{g}}_2(\mathbf{r}, t)$ are known functions at the boundary.

Eq. (1) is an integro-partial-differential equation, and exact closed form solutions for general initial and boundary conditions, Eqs. (3) and (4), are difficult to obtain for most kernel functions. In this paper, the internal and external damping kernel functions are assumed to be separable in space and time, so that,

$$C_i(\mathbf{r}, \xi, t-\tau) = H_i(\mathbf{r})c_i(\mathbf{r}-\xi)g_i(t-\tau) \tag{5a}$$

and

$$C_e(\mathbf{r}, \xi, t-\tau) = H_e(\mathbf{r})c_e(\mathbf{r}-\xi)g_e(t-\tau). \tag{5b}$$

This is the most general form of damping in this study, and represents a non-local viscoelastic damping model. There are three special cases of this general damping model for one-dimensional dynamic systems. The subscripts for the internal and external damping kernels will be removed for the rest of this section, and the following discussion applies equally to both models.

2.1. Viscous damping

Consider a kernel function given by a delta function in both space and time. Thus,

$$C(x, \xi, t-\tau) = H(x)\delta(x-\xi)\delta(t-\tau), \tag{6}$$

where x is the one-dimensional spatial variable and $\delta(\bullet)$ is the Dirac delta function. Physically the spatial delta function means that the damping force is 'locally reacting' and the time delta function implies that the force depends only on the instantaneous value of the velocity or strain rate. This model represents the well-known viscous damping model, however no assumption about proportional damping has been made.

2.2. Viscoelastic damping (time hysteresis)

Suppose that the kernel function is given by a delta function in space but depends on the past time histories via a convolution integral, as described by Eq. (2). The kernel takes the form

$$C(x, \xi, t-\tau) = H(x)\delta(x-\xi)g(t-\tau) \tag{7}$$

and represents a locally reacting viscoelastic damping model. Such models are also called 'time hysteresis' damping.

2.3. Non-local viscous damping (spatial hysteresis)

Now consider a kernel function that is given by a delta function in time but depends on the spatial distribution of the velocities via a convolution integral as described by Eq. (2). The kernel function in this case is given by

$$C(x, \xi, t - \tau) = H(x)c(x - \xi)\delta(t - \tau). \tag{8}$$

This kind of damping model could represent a foam material, for example. Physically this model implies that velocities at different locations within a certain domain can affect the damping force at a given point. This spatial hysteresis is similar to the special damping model proposed by Banks and Inman (1991) and Banks et al. (1994) to describe the damping mechanism for a quasi-isotropic pultruded composite beam.

Generally the function $H(x)$ denotes the presence of non-local damping, and thus $H(x) = H_0$ (constant) if the position x is within the damping patch, and $H(x) = 0$ otherwise. The spatial kernel function, $c(x - \xi)$ in Eqs. (5) and (8), is normalised to satisfy the condition,

$$\int_{-\infty}^{\infty} c(x)\,\mathrm{d}x = 1. \tag{9}$$

Common choices for the kernel function, $c(x - \xi)$, for either internal or external damping, are:

Model 1—exponential decay

$$c(x - \xi) = \frac{\alpha}{2}\mathrm{e}^{-\alpha|x-\xi|}, \tag{10a}$$

Model 2—error function

$$c(x - \xi) = \frac{\alpha}{\sqrt{2\pi}}\mathrm{e}^{-\frac{\alpha^2(x-\xi)^2}{2}}, \tag{10b}$$

Model 3—hat shape

$$c(x - \xi) = \begin{cases} \dfrac{1}{l_0} & \text{for } |x - \xi| \leqslant l_0/2, \\ 0 & \text{otherwise,} \end{cases} \tag{10c}$$

Model 4—triangular shape

$$c(x - \xi) = \begin{cases} \dfrac{1}{l_0}\left(1 - \dfrac{|x - \xi|}{l_0}\right) & \text{for } |x - \xi| \leqslant l_0, \\ 0 & \text{otherwise,} \end{cases} \tag{10d}$$

where α and l_0 are the characteristic parameters of the damping material. Although the functions are different it is useful to define a characteristic length to compare the spatial influence of the kernel models. In Eqs. (10a) and (10b), $c(x - \xi) \to 0$ when $\alpha \to \infty$ while in Eqs. (10c) and (10d), $c(x - \xi) = 0$ when $|x - \xi| > l_0$. Thus l_0 (or $\frac{n}{\alpha}$, for some integer $n \geqslant 1$) is called the *influence distance*. Fig. 1 shows the four kernel functions for typical values of these parameters. Other kernel functions could be used, although the damping matrices (defined later) would have to be obtained by numerical integration.

In this paper the parts of the kernel functions concerned with time, $g(t)$, are assumed to be of the form

$$g(t) = \sum_{r=1}^{M} g_r \mu_r \mathrm{e}^{-\mu_r t}, \tag{11}$$

where μ_r are the relaxation constants of the viscoelastic material for the internal and external damping kernels, that may be determined by curve fitting of the measured mechanical properties of the material.

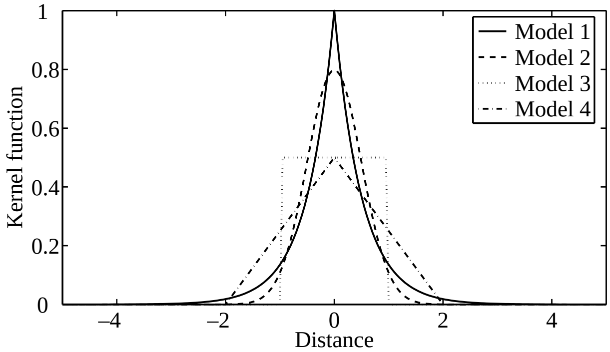

Fig. 1. Four different spatial kernel functions ($l_0 = 2$, $\alpha = 2$).

Other forms of $g(t)$, such as the GHM model (Kim and Kim, 2004; Friswell et al., 1997) may also be analysed using the proposed method. The fractional derivative model (Bagley and Torvik, 1983) is better described in the Laplace domain and is considered in more detail later.

3. The Galerkin solution for a non-local damped beam

Suppose that non-local damping exists for a beam between locations x_1 and x_2, as shown in Fig. 2. These locations could be different for the internal and external damping, but this extension is very straight-forward. The internal damping model is taken as that given by Sorrentino et al. (2003). The equation of motion for this beam may be expressed as the following integro-partial-differential equation,

$$\frac{\partial^2}{\partial x^2}\left(EI(x)\frac{\partial^2 w(x,t)}{\partial x^2}\right) + \rho A(x)\frac{\partial^2 w(x,t)}{\partial t^2} + \int_{x_1}^{x_2}\int_{-\infty}^{t} C_\mathrm{e}(x,\xi,t-\tau)\frac{\partial w(\xi,\tau)}{\partial t}\,\mathrm{d}\tau\,\mathrm{d}\xi + \int_{x_1}^{x_2}\int_{-\infty}^{t} C_\mathrm{i}(x,\xi,t-\tau)\frac{\partial^2}{\partial \xi^2}\left(\gamma(\xi)\frac{\partial^3 w(\xi,\tau)}{\partial \xi^2 \partial \tau}\right)\mathrm{d}\tau\,\mathrm{d}\xi = f(x,t), \tag{12}$$

where $EI(x)$ is the bending stiffness, $\rho A(x)$ is the mass per unit length, $\gamma(x)$ is the internal damping coefficient, $w(x,t)$ is the transverse displacement, and $f(x,t)$ is the distributed external force. In Eq. (12), the third and fourth terms are the non-local external and internal damping. $C_\mathrm{e}(x,\xi,t-\tau)$ and $C_\mathrm{i}(c,\xi,t-\tau)$ are the one-dimensional kernel functions of the form described in the previous section, defined over the spatial sub-domain (x_1,x_2). The appropriate boundary conditions must be satisfied at $x = 0$ and L. For the three simple cases of a clamped, simple supported or free end, the boundary conditions are,

$$\text{Clamped end}\begin{cases} w(x,t) = 0, \\ \dfrac{\partial}{\partial x}w(x,t) = 0. \end{cases} \tag{13a}$$

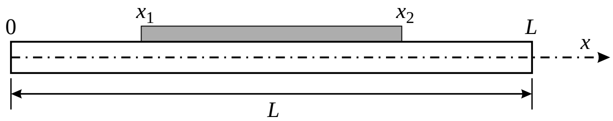

Fig. 2. A beam with a partial non-local damping patch.

$$\text{Simple supported end}\begin{cases} w(x,t) = 0, \\ \dfrac{\partial^2 w(x,t)}{\partial x^2} = 0. \end{cases} \tag{13b}$$

$$\text{Free end}\begin{cases} \dfrac{\partial^2 w(x,t)}{\partial x^2} = 0, \\ \dfrac{\partial}{\partial x}\left[EI(x)\dfrac{\partial^2 w(x,t)}{\partial x^2}\right] = 0. \end{cases} \tag{13c}$$

Taking the Laplace transform of Eq. (12) gives the eigenvalue problem for the free vibration of the beam as

$$\frac{\mathrm{d}^2}{\mathrm{d}x^2}\left(EI(x)\frac{\mathrm{d}^2 W(x,s)}{\mathrm{d}x^2}\right) + s^2\rho A(x)W(x,s) + sG_\mathrm{e}(s)H_0\int_{x_1}^{x_2} c_\mathrm{e}(x-\xi)W(\xi,s)\,\mathrm{d}\xi$$
$$+ sG_\mathrm{i}(s)\int_{x_1}^{x_2} c_\mathrm{i}(x-\xi)\frac{\partial^2}{\partial\xi^2}\left(\gamma(\xi)\frac{\partial^2 W(\xi,s)}{\partial\xi^2}\right)\mathrm{d}\xi = 0, \tag{14}$$

where $G_\mathrm{e}(s)$ and $G_\mathrm{i}(s)$ are the Laplace transforms of the external and internal kernel functions $g_\mathrm{e}(t)$ and $g_\mathrm{i}(t)$, and $W(x,s)$ is the Laplace transform of $w(x,t)$. Eq. (14) is an integro-differential equation, and obtaining closed form solutions is difficult. Approximate solutions will be obtained using the Galerkin method (Fletcher, 1984). The response is approximated by the series,

$$W(x,s) = \sum_{j=1}^{N} q_j(s)\phi_j(x), \tag{15}$$

where $\phi_j(x)$ $(j = 1,2,\ldots,N)$ are given admissible (or trial) functions satisfying the essential boundary conditions, N is the number of admissible functions and is determined by the accuracy required. The admissible functions $\phi_j(x)$ can be chosen in many ways, for example as trigonometric functions, interpolating polynomials, orthogonal polynomials or exponential functions (Fletcher, 1984). A good choice for the beam vibration problem, especially with light damping, is to use the undamped mode shapes.

Substituting $W(x)$ into Eq. (14), multiplying by $\phi_k(x)$ and integrating with respect to x over the length of the beam, gives

$$\left[s^2\mathbf{M} + sG_\mathrm{i}(s)\mathbf{C}_\mathrm{i} + sG_\mathrm{e}(s)\mathbf{C}_\mathrm{e} + \mathbf{K}\right]\mathbf{q} = 0, \tag{16}$$

where $\mathbf{K}$, $\mathbf{M}$, $\mathbf{C}_\mathrm{i}$ and $\mathbf{C}_\mathrm{e}$ are the mass, stiffness and damping (internal and external) matrices with respect to the generalised co-ordinates $\mathbf{q} = \{q_j\}$. The elements of these matrices are given by

$$M_{kj} = \int_0^L \rho A(x)\phi_j(x)\phi_k(x)\mathrm{d}x, \tag{17a}$$

$$C_{\mathrm{e}kj} = H_0\int_{x_1}^{x_2}\int_{x_1}^{x_2} c_\mathrm{e}(x-\xi)\phi_j(\xi)\phi_k(x)\mathrm{d}\xi\,\mathrm{d}x, \tag{17b}$$

$$C_{\mathrm{i}kj} = \int_{x_1}^{x_2}\int_{x_1}^{x_2} c_\mathrm{i}(x-\xi)\frac{\mathrm{d}^2}{\mathrm{d}\xi^2}\left(\gamma(\xi)\frac{\mathrm{d}^2\phi_j(\xi)}{\mathrm{d}\xi^2}\right)\phi_k(x)\mathrm{d}\xi\,\mathrm{d}x, \tag{17c}$$

$$K_{kj} = \int_0^L \frac{\mathrm{d}^2}{\mathrm{d}x^2}\left(EI(x)\frac{\mathrm{d}^2\phi_j(x)}{\mathrm{d}x^2}\right)\phi_k(x)\mathrm{d}x = \int_0^L EI(x)\frac{\mathrm{d}^2\phi_j(x)}{\mathrm{d}x^2}\frac{\mathrm{d}^2\phi_k(x)}{\mathrm{d}x^2}\mathrm{d}x + K^*_{kj}, \tag{17d}$$

where $K^*_{kj} = \left[\frac{\mathrm{d}}{\mathrm{d}x}\left[EI(x)\frac{\mathrm{d}^2\phi_j(x)}{\mathrm{d}x^2}\right]\phi_k(x) - EI(x)\frac{\mathrm{d}^2\phi_j(x)}{\mathrm{d}x^2}\frac{\mathrm{d}\phi_k(x)}{\mathrm{d}x}\right]_0^L$ is a term evaluated at the boundaries produced by the integration by parts. For the three common boundary conditions given in Eq. (13), that is free, simply supported and clamped, $K^*_{kj} = 0$.

The eigenvalues are obtained by solving

$$\det\left|s^2\mathbf{M} + sG_{\mathrm{i}}(s)\mathbf{C}_{\mathrm{i}} + sG_{\mathrm{e}}(s)\mathbf{C}_{\mathrm{e}} + \mathbf{K}\right| = 0. \tag{18}$$

The corresponding mode shape functions are obtained by substituting the eigenvalues into Eq. (16) and computing the null space of the matrix.

In the above analysis, no assumption about proportional damping has been made and thus the state-space description must be used to find the complex eigenvalues and eigenvectors. For three special cases, the eigenproblem is easier to solve.

3.1. Proportional viscous damping

The eigenvalue problem for the undamped free vibration of a uniform beam (EI and ρA are both constant) with classical end conditions is obtained, by setting the damping to be zero in Eq. (14), as

$$EI\frac{\mathrm{d}^4\psi_j(x)}{\mathrm{d}x^4} = \omega_j^2\rho A\psi_j(x), \quad j = 1, 2, \ldots, \infty, \tag{19}$$

where ω_j are the undamped natural frequencies, and $\psi_j(x)$ are corresponding mode shape functions. These mode shape functions satisfy the boundary conditions at 0 and L and also satisfy the following orthogonality relationships

$$\int_0^L \rho A\psi_j(x)\psi_k(x)\mathrm{d}x = \delta_{jk}, \tag{20a}$$

$$\int_0^L EI\frac{\mathrm{d}^2\psi_j(x)}{\mathrm{d}x^2}\frac{\mathrm{d}^2\psi_k(x)}{\mathrm{d}x^2}\mathrm{d}x = \omega_j^2\delta_{jk}. \tag{20b}$$

If these mode shape functions are used as the admissible functions in Eq. (15), then Eq. (16) for the undamped system becomes N decoupled linear equations. A system with proportional damping then becomes

$$(s^2 + sG(s)C_{jj} + \omega_j^2)q_j = 0 \quad (j = 1, 2, \ldots, N), \tag{21}$$

where the damping term C_{jj} can arise from either internal or external damping. Since $q_j \neq 0$,

$$s^2 + sG(s)C_{jj} + \omega_j^2 = 0 \tag{22}$$

and the roots of these equations give the complex eigenvalues s_j of the proportionally damped system. The corresponding undamped mode shapes, $\psi_j(x)$, will also be the mode shapes of the damped system.

For a general, non-proportionally damped system, if the trial functions are taken as the undamped modes, $\psi_j(x)$, then based on the orthogonality relationships, Eq. (20), the mass and stiffness matrices, $\mathbf{M}$ and $\mathbf{K}$, in Eqs. (17a) and (17d) will be diagonal, and only the damping matrices, $\mathbf{C}_{\mathrm{i}}$ and $\mathbf{C}_{\mathrm{e}}$, will be full. This simplifies the analysis, and other forms of trial functions are not usually any more convenient.

For viscous damping (either internal or external), $G(s) = 1$, and using the orthogonality relationships, Eq. (20) for a proportionally damped system can be written as

$$s^2 + sC_{jj} + \omega_j^2 = 0. \tag{23}$$

Since the coefficients of this quadratic equation are real, the eigenvalues occur as complex conjugate pairs, and

$$|s_j|^2 = \mathrm{Re}(s_j)^2 + \mathrm{Im}(s_j)^2 = \omega_j^2. \tag{24}$$

Since C_{jj} is proportional to H_0 in Eq. (17b), as H_0 is increased, the locus of the eigenvalue s_j in the complex plane is a circular arc of radius ω_j. When the damping is close to proportional, and so the non-diagonal elements of the damping matrix may be neglected, the complex eigenvalues of the damped system, $\bar{s}_j$, can be approximated as

$$\bar{s}_j \approx \frac{-C_{jj} \pm \mathrm{i}\sqrt{4\omega_j^2 - C_{jj}}}{2} \tag{25}$$

and the locus of $\bar{s}_j$ would be close to a circular arc.

3.2. Proportional non-viscous damping

For a structure with non-viscous, proportional damping the undamped mode shapes will decouple the equations of motion. The simplest case is when the relaxation function is $G(s) = \frac{\mu}{\mu+s}$, and the eigenproblem becomes

$$s^2 + sG(s)C_{jj} + \omega_j^2 = s^2 + \frac{s\mu}{\mu+s}C_{jj} + \omega_j^2 = 0. \tag{26}$$

In contrast to viscous proportional damping, where one obtains a quadratic equation, Eq. (26) may be written as the cubic equation,

$$\frac{1}{\mu}s^3 + s^2 + \left(C_{jj} + \frac{\omega_j^2}{\mu}\right)s + \omega_j^2 = 0. \tag{27}$$

The three roots of Eq. (27) can have two distinct forms: (a) one root is real and the other two roots form a complex conjugate pair, or (b) all of the roots are real. The complex conjugate pair of roots in case (a) corresponds to an underdamped oscillator that usually arises when the "small damping" assumption is made, while the real root corresponds to a purely dissipative motion. Case (b) represents an overdamped system which cannot sustain any oscillatory motion. For case (a), the locus of the complex conjugate pair of eigenvalues is more complicated than for viscous damping and Adhikari (2005) discusses this in more detail.

For the fractional derivative damping model a typical form of the relaxation function is $G(s) = \frac{E_1 s^{\alpha} - E_0 s^{\beta}}{1+bs^{\beta}}$ for $0 < \alpha, \beta < 1$ (Adhikari, 2000). In this case solving the eigenvalue problem, equivalent to Eq. (26), results in a transcendental equation that may only be solved numerically for increasing damping coefficients. Further analysis of this model is beyond the scope of this paper.

3.3. Small damping

For small damping, Woodhouse (1998) proposed a method that obtained the approximate complex natural frequencies and eigenmodes as

$$\bar{\omega}_j = \omega_j + \mathrm{i}G(\mathrm{i}\omega_j)C_{jj}/2, \tag{28}$$

$$\bar{\phi}_j(x) = \psi_j(x) + \mathrm{i}\sum_{\substack{k=1\\ j\neq k}}^{N} \frac{\omega_j G(\mathrm{i}\omega_j)C_{kj}\psi_k(x)}{\omega_j^2 - \omega_k^2}, \tag{29}$$

where ω_j is the jth undamped natural frequency, and $\psi_j(x)$ is the corresponding mode shape. $\bar{\omega}_j$ and $\bar{\phi}_j(x)$ are the approximations to the jth complex natural frequency and mode shape of the damped system.

4. The Galerkin solution for a plate with non-local damping

Consider the free vibration of a simply supported rectangular plate shown in Fig. 3. The equation of motion is

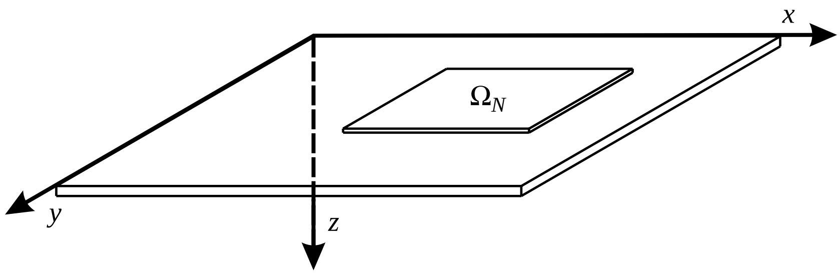

Fig. 3. A rectangular plate with a patch of non-local damping material.

$$D\left(\frac{\partial^4}{\partial x^4}+2\frac{\partial^4}{\partial x^2\partial y^2}+\frac{\partial^4}{\partial y^4}\right)w(x,y,t)+\iint_{\Omega_N}\int_0^t C_e(x,y,\xi,\eta,t-\tau)\frac{\partial w(\xi,\eta,\tau)}{\partial \tau}\,d\tau\,d\xi\,d\eta + \rho h\frac{\partial^2 w(x,y,t)}{\partial t^2}=f(x,y,t), \tag{30}$$

where $w(x,y,t)$ and $f(x,y,t)$ are the transverse deflection and external force, respectively. $D=Eh^3/12(1-\mu^2)$ is the bending stiffness of the plate, h is the thickness, and μ is Possion's ratio. Eq. (30) is similar to Eq. (12), although a uniform plate has been assumed (D and ρh are constant). Only external non-local damping is considered, and an equivalent term for internal damping, similar to that for the beam, could be defined. Kernel functions equivalent to those of the plate may be defined, although closed form expressions for the damping matrices, equivalent to Eq. (17), are only possible for two of the models. Other kernel functions could be used, although the damping matrices would have to be obtained by numerical integration. The kernel function is assumed to be separable and may be written as,

$$C_e(x,y,\xi,\eta,t)=H(x,y)c(x,y,\xi,\eta)g(t). \tag{31}$$

The function $H(x,y)=H_0$ (constant) within the damping patch and zero otherwise. The models for the spatial kernel function, $c(x,y,\xi,\eta)$, used in this paper are

Model 1—exponential decay

$$c(x,y,\xi,\eta)=\frac{\alpha^2}{2\pi}e^{-\alpha d}. \tag{32a}$$

Model 2—error function

$$c(x,y,\xi,\eta)=\frac{\alpha^2}{2\pi}e^{-\alpha^2\frac{d^2}{2}}, \tag{32b}$$

where $d=\sqrt{(x-\xi)^2+(y-\eta)^2}$ is the distance between two points (x,y) and (ξ,η).

Taking the Laplace transform of Eq. (30) gives the eigenvalue problem for the free vibration of the plate with non-local external damping as

$$D\left(\frac{\partial^4}{\partial x^4}+2\frac{\partial^4}{\partial x^2\partial y^2}+\frac{\partial^4}{\partial y^4}\right)W(x,y,s)+sG(s)\iint_{\Omega_N} C_e(x,y,\xi,\eta,t-\tau)W(\xi,\eta,s)\,d\xi\,d\eta + s^2\rho hW(x,y,s)=0. \tag{33}$$

The response is written as a summation of admissible functions,

$$W(x,y,s)=\sum_{j=1}^{N}q_j(s)\phi_j(x,y). \tag{34}$$

Substituting this expression for $W(x, y, s)$ into Eq. (33), multiplying by $\phi_k(x, y)$ and performing the integration $\int\int_{\Omega_N}(\cdot)\,\mathrm{d}x\,\mathrm{d}y$, produces the standard equation of motion, Eq. (16). However, the elements of the **M**, **K** and $\mathbf{C}_\mathrm{e}$ matrices for the plate problem are

$$M_{kj} = \rho h \iint_{\Omega_N} \phi_j(x,y)\phi_k(x,y)\,\mathrm{d}x\,\mathrm{d}y \tag{35a}$$

$$C_{\mathrm{e}kj} = H_0 \iint_{\Omega_N} \iint_{\Omega_N} c_\mathrm{e}(x,y,\xi,\eta)\phi_k(x,y)\phi_j(\xi,\eta)\,\mathrm{d}\xi\,\mathrm{d}\eta\mathrm{d}x\,\mathrm{d}y \tag{35b}$$

$$K_{kj} = D \iint_{\Omega_N} \phi_k(x,y)\left(\frac{\partial^4}{\partial x^4} + 2\frac{\partial^4}{\partial x^2 \partial y^2} + \frac{\partial^4}{\partial y^4}\right)\phi_j(x,y)\,\mathrm{d}x\,\mathrm{d}y \tag{35c}$$

$$= D \iint_{\Omega_N} \left(\frac{\partial^2\phi_j(x,y)}{\partial x^2} + \frac{\partial^2\phi_j(x,y)}{\partial y^2}\right)\left(\frac{\partial^2\phi_k(x,y)}{\partial x^2} + \frac{\partial^2\phi_k(x,y)}{\partial y^2}\right)\mathrm{d}x\,\mathrm{d}y + \overline{K}^*_{kj}, \tag{35d}$$

where $\bar{K}^*_{kj}$ is zero for the classical free, simply supported and clamped boundary conditions.

5. Numerical examples

5.1. A simply supported beam with a non-local damping patch

A simply supported homogeneous beam, shown in Fig. 4, has length $L = 2$ m, width $b = 0.005$ m, thickness $h = 0.005$ m, Young's modulus $E = 70$ GPa and mass density $\rho = 2700$ kg/m^3. The positions of the left and right ends of the non-local damping patch are $x_1 = L/4$, $x_2 = 3L/4$, respectively. The admissible functions are taken as the first seven mode shape functions of the undamped beam, so that,

$$W(x,s) = \sum_{j=1}^{7} q_j(s)\sqrt{\frac{2}{\rho AL}}\sin\frac{j\pi x}{L}. \tag{36}$$

Although other admissible functions could be used, the undamped mode shapes are convenient and efficient, especially when the damping is light. Since the undamped mode shapes are used, Eq. (17) produces diagonal mass and stiffness matrices, $\mathbf{M} = \mathbf{I}_{7\times7}$ and $\mathbf{K} = \mathrm{diag}(\omega_j^2)$. Of course the external and internal damping matrices, $\mathbf{C}_\mathrm{e}$ and $\mathbf{C}_\mathrm{i}$, are not diagonal and the non-zero elements must be computed using either closed form expressions or by numerical integration.

Tables 1 and 2 compare the lowest five eigenvalues for the four different spatial kernel functions and two different time kernel function parameter sets, for external non-local damping. The first case is for a non-local viscous damping model (i.e. $\mu = \infty$ or $g(t) = \delta(t)$) and the second case is for a non-viscous damping model (i.e. $\mu = 20$ or $g(t) = 20\mathrm{e}^{-20t}$). In Tables 1 and 2, the approximate eigenvalues of the beam with non-local damping are computed by two methods, namely the Galerkin method and Woodhouse's method.

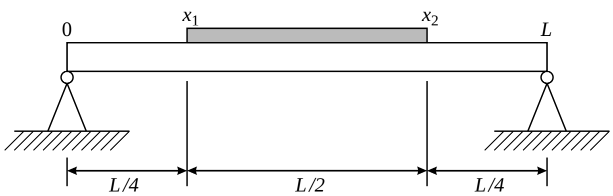

Fig. 4. The simply supported beam with a non-local damping patch.

Table 1
The first five eigenvalues of the simply supported beam with non-local, viscous external damping

Method	Mode no.	Model 1	Model 2	Model 3	Model 4
$L = 2.0$, $\mu = \infty$, $H_0 = 2.0$, $\alpha = 5$, $l_0 = 0.8$					
Galerkin method	1	−9.9601 ± 15.184i	−10.506 ± 14.818i	−10.034 ± 15.139i	−9.0941 ± 15.712i
	2	−3.7798 ± 72.459i	−4.2737 ± 72.439i	−3.3654 ± 72.475i	−2.2865 ± 72.506i
	3	−3.0263 ± 162.95i	−3.3134 ± 162.90i	−2.5091 ± 162.93i	−1.8845 ± 163.01i
	4	−3.5684 ± 290.03i	−4.0318 ± 290.00i	−2.7349 ± 290.05i	−1.7541 ± 290.11i
	5	−2.5893 ± 453.32i	−2.627 ± 453.32i	−0.6004 ± 453.34i	−0.6003 ± 453.34i
Woodhouse method	1	−9.9318 ± 18.134i	−10.470 ± 18.134i	−10.003 ± 18. 134i	−9.0736 ± 18.134i
	2	−3.7775 ± 72.535i	−4.2702 ± 72.535i	−3.3637 ± 72.535i	−2.2861 ± 72.535i
	3	−3.0545 ± 163.20i	−3.3487 ± 163.20i	−2.5410 ± 163.20i	−1.9049 ± 163.20i
	4	−3.5707 ± 290.14i	−4.0351 ± 290.14i	−2.7366 ± 290.14i	−1.7545 ± 290.14i
	5	−2.5894 ± 453.34i	−2.6269 ± 453.34i	−0.6004 ± 453.34i	−0.6004 ± 453.34i

Table 2
First five eigenvalues of the simply supported beam with non-local, viscoelastic external damping

Method	Mode no.	Model 1	Model 2	Model 3	Model 4
$L = 2.0$, $\mu = 20$, $H_0 = 2.0$, $\alpha = 5$, $l_0 = 0.8$					
Galerkin method	1	−4.7317 ± 24.564i	−4.9012 ± 24.959i	−4.7527 ± 24.616i	−4.4395 ± 23.935i
	2	−0.26010 ± 73.498i	−0.29300 ± 73.623i	−0.23225 ± 73.393i	−0.15905 ± 73.119i
	3	−0.045816 ± 163.57i	−0.050285 ± 163.61i	−0.038394 ± 163.51i	−0.028769 ± 163.44i
	4	−0.016916 ± 290.38i	−0.019122 ± 290.42i	−0.012971 ± 290.33i	−0.0083093 ± 290.26i
	5	−0.0050294 ± 453.46i	−0.0051020 ± 453.46i	−0.0011664 ± 453.37i	−0.0011666 ± 453.37i
Woodhouse method	1	−5.4508 ± 23.076i	−5.7463 ± 23.344i	−5.4897 ± 23.111i	−4.9798 ± 22.649i
	2	−0.26690 ± 73.503i	−0.30171 ± 73.629i	−0.23766 ± 73.397i	−0.16152 ± 73.121i
	3	−0.045193 ± 163.57i	−0.049545 ± 163.61i	−0.037595 ± 163.51i	−0.028183 ± 163.43i
	4	−0.016887 ± 290.38i	−0.019083 ± 290.42i	−0.012942 ± 290.33i	−0.0082975 ± 290.26i
	5	−0.0050299 ± 453.46i	−0.0051028 ± 453.46i	−0.0011663 ± 453.37i	−0.0011663 ± 453.37i

Numerical results show that the results from the proposed method are very close to those obtained by Woodhouse's method for the second to fifth complex eigenvalues. For the first eigenvalue, Woodhouse's method is not appropriate since the damping ratio is high. The Woodhouse approach gives identical imaginary parts for all of eigenvalues from different spatial kernels for the viscous damping model ($\mu = \infty$), although the imaginary parts are different for non-viscous damping because $G(i\omega_j)$ is complex. Using the proposed method, model 2 has the largest damping ratios for the first five eigenvalues, while model 4 has the smallest damping ratio.

Figs. 5 and 6 show the effects of the four different spatial kernels on the real and imaginary parts of the first four complex modes for external damping. The influence of the length parameter α in the spatial kernel function on the damping ratios of the first five modes is shown in Fig. 7, for a time hysteresis parameter of $\mu = \infty$. All of the damping ratios are very sensitive for small values of α and approach steady values for large α, with a fixed damping coefficient H_0. Fig. 8 shows the root locus of the first eigenvalue of the beam for different values of α when H_0 increases from 0 to 2.68082 N s m^{-2} for viscous damping ($\mu = \infty$) and non-local viscous external damping with the kernel function given by model 1. For higher values of H_0 the mode becomes overdamped. The root locus is very close to a circular arc, and this implies that the non-local damping model in this example is close to proportional for first mode. Sorrentino et al. (2003) also found nearly coincident root locus curves for the low modes of a homogeneous beam with proportional and non-proportional damping.

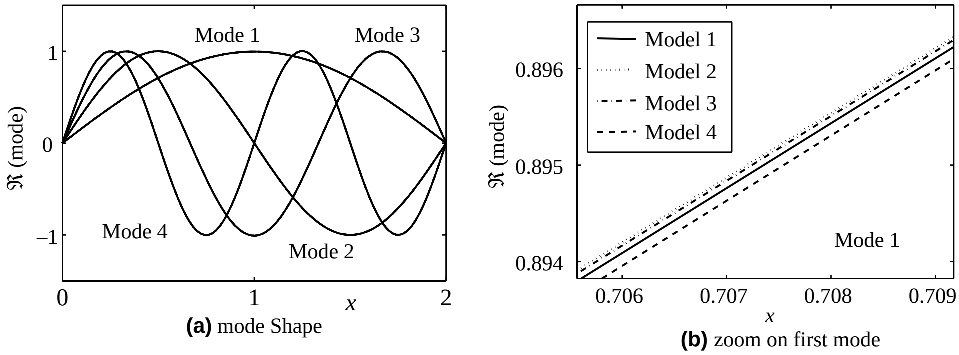

Fig. 5. The real parts of the first four mode shapes of the simply supported beam with non-local, viscoelastic external damping. (a) Mode shape and (b) zoom on first mode.

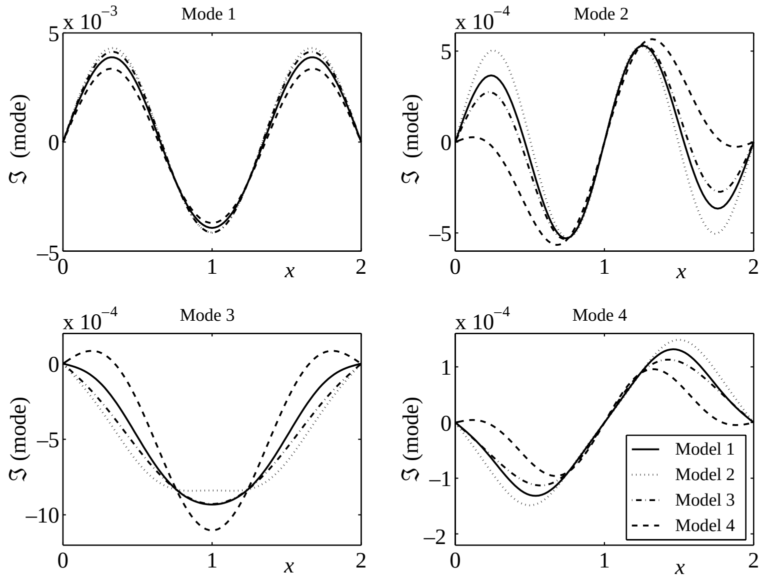

Fig. 6. The imaginary parts of the first four mode shapes of the simply supported beam with non-local, viscoelastic external damping.

Fig. 9 shows the effect of changing the patch position on the damping ratios of the first five modes, while maintaining the same patch length. The position is defined using the left end of the patch, x_1. The damping ratios of modes 1 and 2 increase monotonically when the left end of the non-local damping patch moves from the left end of the beam to the centre (x_1 changes from 0 to 0.5), while the damping ratios of the third and fourth modes have a peak for a certain patch position. The damping ratio of the fifth mode is small and nearly constant.

Fig. 10 shows the root locus for the first four modes with a non-local internal damping model and $\mu = \infty$. Here, the internal damping coefficient $\gamma(x)$ is assumed to be a constant, γ_0, and increases from 0 to 1 N s m^2. The first and the second modes never reach the real axis and hence remain underdamped, whereas the third and forth modes become overdamped for a certain value of γ_0. The loci are not circular arcs because the damping is not proportional.

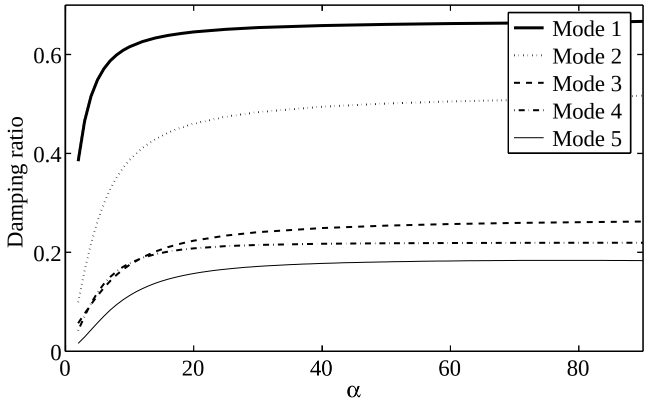

Fig. 7. The effect of the parameter α on the damping ratios of the first five modes (external damping, model 1 kernel function, $\mu = \infty$; $H_0 = 1$ for mode 1, $H_0 = 5$ for mode 2, $H_0 = 10$ for other modes).

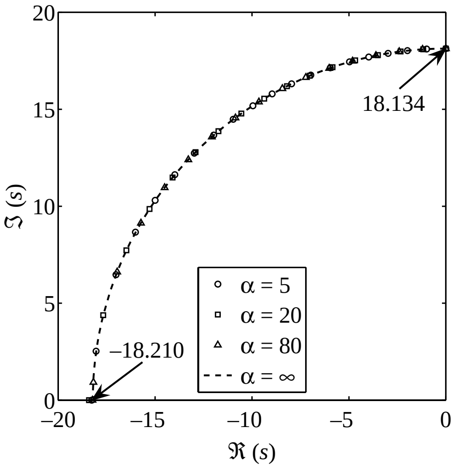

Fig. 8. The root locus of the first eigenvalue with a non-local external damping patch as H_0 increases from 0 to 2.68028 (for $\mu = \infty$).

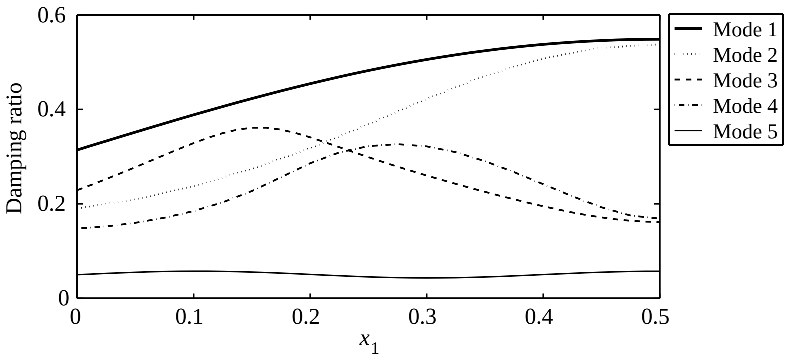

Fig. 9. The effect of patch position on the damping ratios of the first five modes (external damping, model 1 kernel function, with $\alpha = 5$, $\mu = \infty$; $H_0 = 1$ for mode 1, $H_0 = 10$ for other modes).

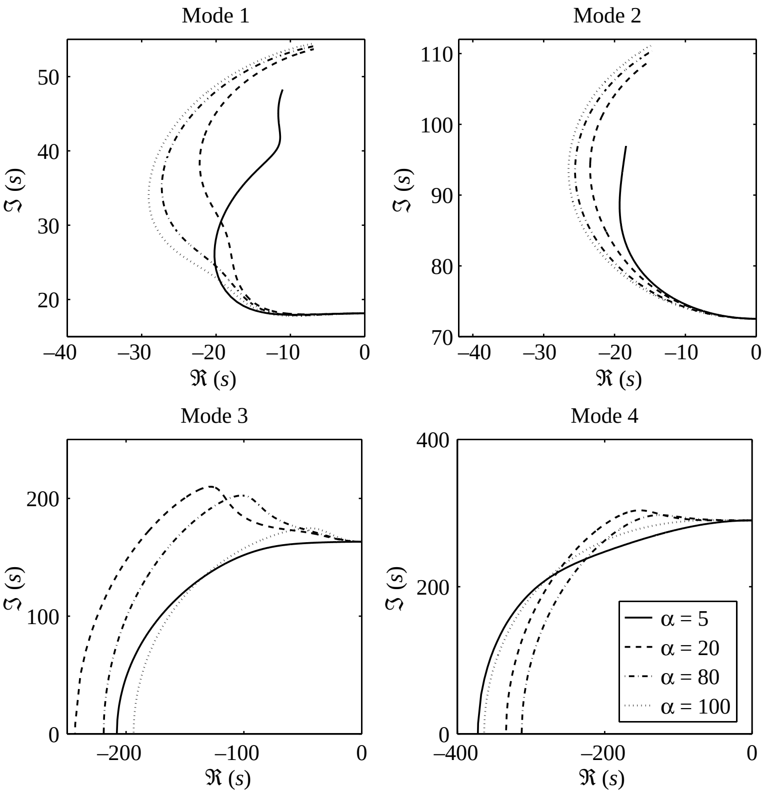

Fig. 10. The root loci of the first four eigenvalues with non-local internal damping ($\mu = \infty$, γ_0 increases from 0 to 1 N s m^2).

5.2. A cantilever beam with non-local damping

Fig. 11 shows a cantilever beam with a non-local damping patch. The properties of the beam are identical to those for the simply supported example. The admissible functions are taken as the first seven mode shape functions of an undamped cantilever beam, so that,

$$W(x,s) = \sum_{j=1}^{7} q_j(s)\sqrt{\frac{1}{\rho AL}}\left[\cosh\beta_j x - \cos\beta_j x - \frac{\cosh\beta_j L + \cos\beta_j L}{\sinh\beta_j L + \sin\beta_j L}\left(\sinh\beta_j x - \sin\beta_j x\right)\right], \tag{37}$$

where $\beta_j L$ are the roots of the frequency equation for the undamped cantilever beam,

$$1 + \cos\beta L\cosh\beta L = 0. \tag{38}$$

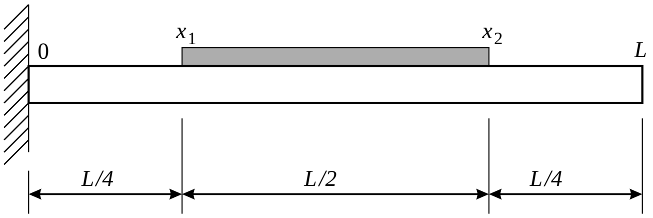

Fig. 11. The cantilever beam with non-local damping.

The roots of Eq. (38) are obtained numerically, and the first four solutions are $\beta_j L = 1.8751$, 4.6941, 7.8548 and 10.996.

Table 3 gives the eigenvalues for the four different spatial kernel functions, for viscous and non-viscous time kernels and external damping. Figs. 12 and 13 show the real and imaginary parts of the first four mode shapes. Note that the real parts of the modes are very similar to the undamped mode shapes and the imaginary parts are relatively small.

5.3. A simply supported plate with a non-local damping patch

Consider an isotropic rectangular plate with uniform thickness h, with its mid-surface lying in the x–y plane and bounded by the edges $x = 0$, a and $y = 0$, b, as shown in Fig. 14. The non-local external damping patch is positioned in the middle of the plate. Two plates are considered, a square plate of length 2 m, and a rectangular plate of dimensions 2 m × 4 m, both with thickness $h = 0.005$ m, Young's modulus $E = 70$ GPa, mass density $\rho = 2700$ kg/m^3 and Poisson's ratio $\mu = 0.3$. The admissible functions are taken as the mode shape functions of an undamped, simply supported plate,

Table 3
The first five eigenvalues of the cantilever beam with non-local external damping ($L = 2.0$, $H_0 = 2.0$, $\alpha = 5$, $l_0 = 0.8$)

Mode no.	Model 1	Model 2	Model 3	Model 4
Viscous, $\mu = \infty$				
1	−3.4999 ± 5.6562i	−3.7195 ± 5.5421i	−3.4418 ± 5.6992i	−3.0522 ± 5.8768i
2	−8.0368 ± 38.520i	−8.5142 ± 38.286i	−8.1328 ± 38.461i	−7.2758 ± 38.836i
3	−4.5634 ± 113.24i	−5.1781 ± 113.21i	−4.0529 ± 113.27i	−2.7151 ± 113.31i
4	−2.5122 ± 222.04i	−2.7386 ± 222.02i	−1.5613 ± 222.03i	−1.0309 ± 222.07i
5	−2.7293 ± 367.13i	−2.9913 ± 367.11i	−1.6382 ± 367.15i	−1.1165 ± 367.19i
Viscoelastic, $\mu = 20$				
1	−4.2092 ± 8.0111i	−4.5115 ± 8.2667i	−4.0864 ± 7.9676i	−3.5140 ± 7.6256i
2	−1.5841 ± 43.908i	−1.6750 ± 44.126i	−1.6027 ± 43.951i	−1.4407 ± 43.566i
3	−0.13619 ± 114.14i	−0.15426 ± 114.24i	−0.12115 ± 114.05i	−0.081473 ± 113.82i
4	−0.020349 ± 222.36i	−0.022217 ± 222.38i	−0.012764 ± 222.28i	−0.0084141 ± 222.23i
5	−0.0080918 ± 367.36i	−0.0088757 ± 367.37i	−0.0048627 ± 367.30i	−0.0033079 ± 367.27i

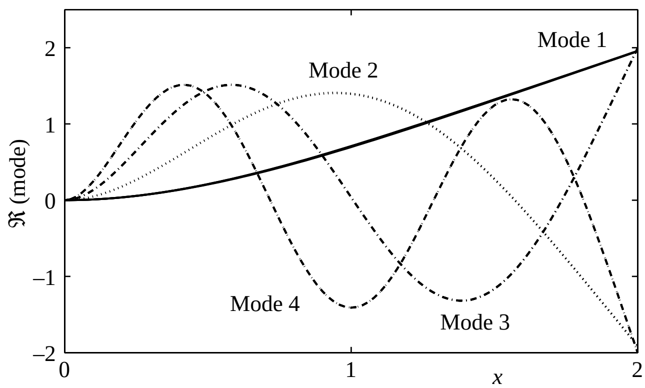

Fig. 12. The real parts of the first four mode shapes of the cantilever beam with non-local, viscoelastic external damping.

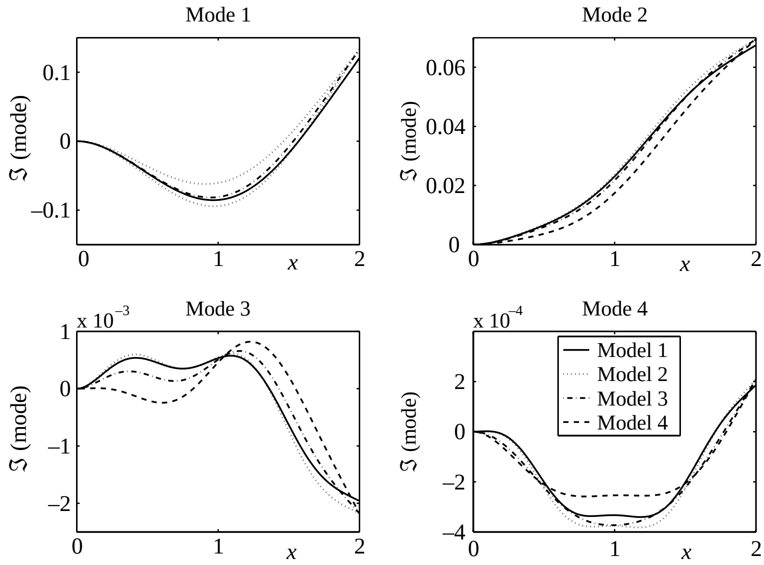

Fig. 13. The imaginary parts of the first four mode shapes of the cantilever beam with non-local, viscoelastic external damping.

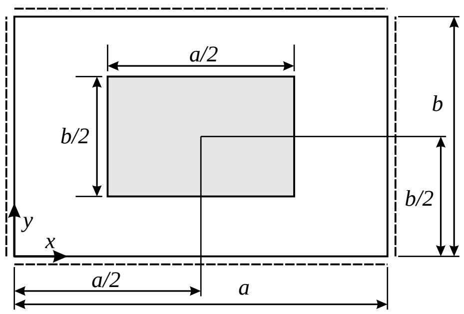

Fig. 14. The simply supported plate with a non-local damping patch.

$$W(x,y,s) = \frac{2}{\sqrt{\rho a b h}} \sum_{m=1}^{N_1} \sum_{n=1}^{N_2} q_{mn}(s) \sin\frac{m\pi x}{a} \sin\frac{n\pi y}{b}. \tag{39}$$

Comparing Eq. (39) with Eq. (34) shows that $N = N_1 \times N_2$, and the mode shapes in Eq. (39) may be indexed by increasing natural frequency. Substituting Eq. (39) into Eq. (35), produces diagonal mass and stiffness matrices, and a non-diagonal damping matrix. The generalised co-ordinate vector is $\mathbf{q} = [q_{11}, q_{12}, \ldots, q_{1N_2}, q_{21}, q_{22}, \ldots, q_{N_1N_2}]^{\mathrm{T}}$.

Table 4 shows the nine complex eigenvalues of plate with non-local viscous damping, for the square and rectangular plates. Only nine admissible functions were used ($N_1 = N_2 = 3$). The damping is relatively light and both damping models give similar imaginary parts for the eigenvalues. The location of the patch also means that the first mode is most heavily damped. Fig. 15 shows the root locus for the first four modes as H_0 is increased from 0 to 8×10^3 N s m^{-3} for the rectangular plate. Only the third mode remains underdamped, while the other three modes become overdamped for certain values of H_0, which are different for each mode. The loci for mode 1 are very close to circular showing that the first mode is almost proportionally

Table 4
The nine complex eigenvalues of the plate with non-local external damping ($H_0 = 400.0$, $\alpha = 10$, $\mu = \infty$)

Mode no. (m,n)	Model 1	Model 2
$a = b = 2.0$		
(1,1)	−8.0107 ± 37.223i	−8.8005 ± 37.055i
(1,2)	−3.7020 ± 95.010i	−4.5783 ± 94.991i
(1,3)	−1.3789 ± 190.10i	−1.9714 ± 190.10i
(2,1)	−3.7020 ± 95.010i	−4.5783 ± 94.991i
(2,2)	−1.7553 ± 152.08i	−2.3857 ± 152.08i
(2,3)	−1.3949 ± 247.13i	−1.9084 ± 247.13i
(3,1)	−1.3789 ± 190.10i	−1.9714 ± 190.10i
(3,2)	−1.3949 ± 247.13i	−1.9084 ± 247.13i
(3,3)	−1.1048 ± 342.13i	−1.5208 ± 342.12i
$a = 2$, $b = 4.0$		
(1,1)	−8.7643 ± 22.320i	−9.2658 ± 22.133i
(1,2)	−4.7290 ± 37.926i	−5.2456 ± 37.898i
(1,3)	−3.6029 ± 61.267i	−3.9978 ± 61.238i
(2,1)	−3.9825 ± 80.781i	−4.7493 ± 80.775i
(2,2)	−2.1873 ± 95.089i	−2.7066 ± 95.109i
(2,3)	−1.7402 ± 118.74i	−2.1548 ± 118.72i
(3,1)	−3.1374 ± 175.65i	−3.7679 ± 175.65i
(3,2)	−1.7295 ± 190.03i	−2.1549 ± 190.03i
(3,3)	−1.3711 ± 213.74i	−1.7106 ± 213.71i

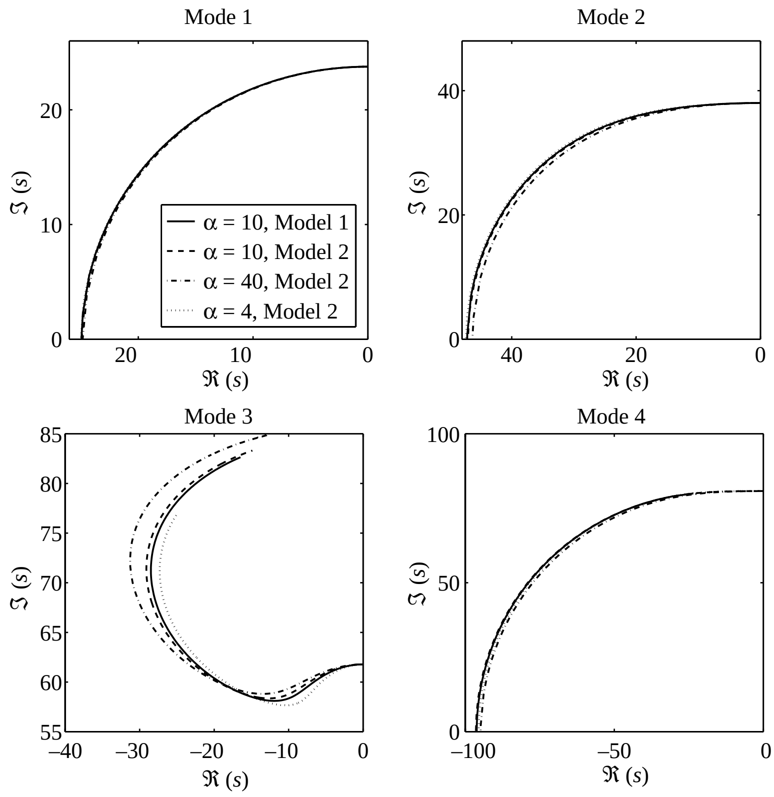

Fig. 15. The root loci of first four eigenvalues of the simply supported rectangular plate with external damping as H_0 increases from 0 to 8×10^3 (for $\mu = \infty$).

damped. The loci for modes 2 and 4 are close to circular, showing a small level of non-proportionality, and mode 3 is highly non-proportional.

6. Conclusions

In this paper, a non-local damping model for distributed parameter systems has been proposed and analysed. This damping model is a generalisation of the linear viscous damping model, where the damping force at a given point depends on the time history and the velocities within a spatial domain. Approximate solutions have been obtained for beam and plate systems with non-local damping patches, using the Galerkin method. The influence of different non-local damping kernel functions on the dynamic characteristics of the beam and plate structures has been investigated. It has been demonstrated that the damping model has a significant impact on the damping ratios of the modes of a structure. The next stage is to use the modelling and analysis tools developed here to optimise the damping in structures, by considering the non-local nature of the damping material, as well as its location and thickness.

Acknowledgement

Yongjun Lei gratefully acknowledges the support of China Scholarship Council through a Scholarship Fund Award. Michael Friswell gratefully acknowledges the support of the Royal Society through a Royal Society-Wolfson Research Merit Award. Sondipon Adhikari gratefully acknowledges the support of the Engineering and Physical Sciences Research Council through the award of an Advanced Research Fellowship.

References

Adhikari, S., 2000. Damping models for structural vibrations. Ph.D. Thesis, Cambridge University, UK.

Adhikari, S., 2001. Eigenrelations for nonviscously damped system. AIAA Journal 39 (8), 1624–1630.

Adhikari, S., 2005. Qualitative dynamic characteristics of a non-viscously damped oscillator. Proceedings of the Royal Society of London Series A 461 (2059), 2269–2288.

Adhikari, S., Woodhouse, J., 2001. Identification of damping. Part 2: Non-viscous damping. Journal of Sound and Vibration 243 (1), 63–88.

Adhikari, S., Lei, Y., Friswell, M.I., Dynamic of non-viscously damped beams. Journal of Applied Mechanics, submitted for publication.

Agrawal, O.P., 2004. Analytical solution for stochastic response of a fractionally damped beam. Journal of Vibration and Acoustics 126 (4), 561–566.

Ahmadi, G., 1975. Linear theory of nonlocal viscoelasticity. International Journal of Non-Linear Mechanics 10 (2), 253–258.

Atanackovic, T.M., Stankovic, B., 2004. Stability of an elastic rod on a fractional derivative type of foundation. Journal of Sound and Vibration 277 (1), 149–161.

Bagley, R.L., Torvik, P.J., 1983. Fractional calculus—a different approach to the analysis of viscoelastically damped structures. AIAA Journal 21 (5), 741–748.

Bagley, R.L., Torvik, P.J., 1985. Fractional calculus in the transient analysis of viscoelastically damped structures. AIAA Journal 23 (6), 918–925.

Banks, H.T., Inman, D.J., 1991. On damping mechanisms in beams. Journal of Applied Mechanics 58 (3), 716–723.

Banks, H.T., Wang, Y., Inman, D.J., 1994. Bending and shear damping in beams—frequency-domain estimation techniques. Journal of Vibration and Acoustics 116 (2), 188–197.

Enelund, M., Josefson, B.L., 1997. Time-domain finite element analysis of viscoelastic structures with fractional derivatives constitutive relations. AIAA Journal 35 (10), 1630–1637.

Eringen, A.C., Edelen, D.G.B., 1972. Nonlocal elasticity. International Journal of Engineering Science 10 (3), 233–248.

Fenander, A., 1998. A fractional derivative railpad model included in a railway track model. Journal of Sound and Vibration 212 (5), 889–903.

Fletcher, C.A.J., 1984. Computational Galerkin Methods. Springer-Verlag, New York.
Flugge, W., 1975. Viscoelasticity, second revised edition. Springer-Verlag, Berlin, p. 74.
Friswell, M.I., Inman, D.J., Lam, M.J., 1997. On the realisation of GHM models in viscoelasticity. Journal of Intelligent Material Systems and Structures 8 (11), 986–993.
Ghoneim, H., 1997. Fluid surface damping versus constrained layer damping for vibration suppression of simply supported beams. Smart Materials and Structures 6 (1), 40–46.
Kim, T.-W., Kim, J.-H., 2004. Eigensensitivity based optimal distribution of a viscoelastic damping layer for a flexible beam. Journal of Sound and Vibration 273 (1–2), 201–218.
Krenk, S., 2004. Complex modes and frequencies in damped structural vibrations. Journal of Sound and Vibration 270 (4–5), 981–996.
Krenk, S., Hogsberg, J.R., 2005. Damping of cables by a transverse force. Journal of Engineering Mechanics 131 (4), 340–348.
Lin, T., Russell, D.L., 2001. A superconvergent method for approximating the bending moment of elastic beam with hysteresis damping. Applied Numerical Mathematics 38 (1–2), 145–165.
Maia, N.M.M., Silva, J.M.M., Ribeiro, A.M.R., 1998. On a general model for damping. Journal of Sound and Vibration 218 (5), 749–767.
Mainardi, F., 1997. Fractional calculus: some basic problems in continuum and statistical mechanics. In: Carpinteri, A., Mainardi, F. (Eds.), Fractals and Fractional Calculus in Continuum Mechanics. Springer Verlag, New York, pp. 291–348.
Nowinski, J.L., 1986. On the non-local aspects of stress in a viscoelastic medium. International Journal of Non-Linear Mechanics 21 (6), 439–446.
Pisno, A.A., Fuschi, P., 2003. Closed form solution for non-local elastics bar in tension. International Journal of Solids and Structures 40 (1), 13–23.
Podlubny, I., 1999. Fractional Differential Equations. Academic Press, New York.
Polizzotto, C., 2001. Non-local elasticity and related variational principles. International Journal of Solids and Structures 38 (42–43), 7359–7380.
Russell, D.L., 1992. On mathematical models for the elastic beam with frequency-proportional damping. In: Banks, H.T. (Ed.), Control and Estimation in Distributed Parameter Systems. SIAM, Philadelphia, PA, pp. 125–169.
Silling, S.A., Zimmermann, M., Aberyaratne, R., 2003. Deformation of a peridynamic bar. Journal of Elasticity 73 (1–3), 173–190.
Sorrentino, S., Marchesiello, S., Piombo, B.A.D., 2003. A new analytical technique for vibration analysis of non-proportionally damped beams. Journal of Sound and Vibration 265 (4), 765–782.
Weckner, O., Abeyaratne, R., 2005. The effect of long-range forces on the dynamics of a bar. Journal of the Mechanics and Physics of Solids 53 (3), 705–728.
Woodhouse, J., 1998. Linear damping models for structural vibration. Journal of Sound and Vibration 215 (3), 547–569.
Yang, B., Tan, C.A., 1992. Transfer functions of one-dimensional distributed parameter systems. Journal of Applied Mechanics 59 (4), 1009–1014.
Yang, B., Wu, X., 1997. Transient response of one-dimensional distributed systems: a closed form eigenfunction expansion realization. Journal of Sound and Vibration 208 (5), 763–776.